Pergamon

Cement and Concrete Research, Vol. 25, No. 5, pp. 969-979, 1995

0008-8846/95 $9.50+.00

0008-8846(95)00092-5

SHEAR BEHAVIOR OF FERROCEMENT THIN WEBBED SECTIONS

S.F. Ahmad, Sarosh H. Lodi, and Juneid Qureshi
Civil Engineering Department
NED University of Engineering & Technology
Karachi-75270, Pakistan

(Refereed)
(Received April 1, 1994; in final form May 3, 1995)

ABSTRACT

The shear behavior of ferrocement channel beams have been studied by conducting tests under transverse loads for 15 beam specimens. Influence of variations of the dominant parameters were studied through systematic tests. Test results indicate that cracking and ultimate shear strength increases with the increase in the volume of wire mesh and mortar strength, and decreases with the increase of shear span to depth ratio. A computational model based on cracking criteria related to combined stresses and ferrocement tensile strength profile distribution across beam depth has been proposed to predict the cracking strength. Also an empirical expression has been developed for the same for ease in direct design application.

Introduction

With the rapid progress of innovative construction technique, application of ferrocement (FC) is increasingly becoming more common for use in various structural engineering applications. This has a led to a large scale research on this material and the presence of a considerable volume of technical information regarding design, construction, maintenance and rehabilitation techniques using ferrocement.

Although most aspects of ferrocement material and structural behavior are being investigated and modelled, with varying degrees of success [1,2,3,4,5,6], the in-plane shear behavior has received comparatively less attention [7,8,9,10]. This may be primarily due to the application range of ferrocement where structural elements, due to there cross-sectional geometry and member span configurations are predominantly subjected to flexural distress, rather than shear. However, transverse shear may be one of the critical design considerations for thin webbed ferrocement beams, where failure mode mechanics might necessitate shear failure prior to flexural failure. With recent developments in the scope of application of ferrocement and the increasing use of flanged ferrocement member cross-sections, such as box beams, channel sections and sandwich ribbed plates, the behavior of the material under transverse shear needs more attention in future research studies.

Sulaimani et al. [7] have studied the behavior of ferrocement under direct shear by conducting axial compression tests on Z-shaped specimens reinforced with woven wire mesh. Results indicate that under direct shear ferrocement exhibits two stages of behavior (cracked and uncracked). Mansur and Ong [8] have studied the shear behavior of rectangular beams under third point loading, varying

different influencing parameters. Results indicate that the cracking strength of ferrocement increases, as shear span to depth ratio decreases and volume fraction and compressive strength of mortar increases. Mansur and Ong [9] have also studied shear strength behavior of ferrocement I-beams and concluded that ultimate shear strength varies similarly with the influencing parameters as the cracking shear strength. Sulaimani et al. [10] have tested ferrocement box beams, by varying the three basic influencing parameters and have observed similar behavior as [8,9]. They have also proposed an empirical expression to compute the cracking shear strength of ferrocement box beams.

As mentioned earlier, the data available for formulating a rational design basis is scant in case of shear. For such a state it is more logical as a first step, to validate the already existing data and to identify areas where improvement is needed. Simultaneously formulation of simplified approaches without under estimating the true material behavior should then be developed. The objective of the said research is therefore, based on the same grounds.

In reinforced concrete structures a much higher probability is often acceptable for serviceability limit mainly because of economy, crack width for different exposure conditions is therefore the established criteria followed by almost every code of practice. Keeping in view the much improved cracking bahavior of ferrocement, it would be quite appropriate to define a general lower limit based on crack free surface. This would simplify the code procedures without resulting in high demands. It should also be noted that ferrocement being relatively more ductile than reinforced concrete, would need more flexural rigidity to function properly, and the lower limit imposed by virtue of first crack stress would also help in fulfilling the deflection criteria.

As channel shaped cross sections have the most practical range of utility this research therefore, reports an experimental study on channel shaped ferrocement specimens under bending and transverse shear and present a simple computational model to predict the first cracking strength, either flexural or web-shear, of generic ferrocement sections based on the classical beam theory. The distribution of flexural and shear stresses are based on homogenous beam concept. The model uses a critical crack criteria based on the tensile stress variation across the depth of the beam. Also an empirical equation is proposed to predict the shear cracking strength of ferrocement for design use purposes.

Experimental Program

To study the shear behavior of ferrocement thin webbed specimens, fifteen channel beams, as shown in Figure 1, were tested.

The parameters varied were the shear span to depth ratio, 'a/h', the volume fraction of the reinforcement, 'V_f' and the strength of the mortar, f'_c. The range of these variations were as follows: a/h, from 1.5 to 2.5; V_f, in the form of wire mesh layers, from one layer to three layers; f'_c, in the form of water-cement ratio, from 0.45 to 0.5. The materials used for casting the ferrocement beams, included ordinary Portland cement, beach dune sand and square woven mesh of 6.25mm opening and 0.95mm diameter. Four No. 4 bars were used as flexural reinforcement. The length of the beams varied from 1m to 1.5m. Transverse stiffeners built into the formwork were provided across the span length.

The test set-up and loading arrangement, as shown in Figure 1, consisted of loading the ferrocement specimens under symmetrical two point loading, varied to obtain the required shear span to depth ratio. An Universal Testing Machine with 30 ton capacity was used for loading the specimens from the top and deflections at center point, and 150mm on either side of the centers, were measured through

LVDT's. During testing the initiation of cracks was carefully monitored and the crack pattern of each beam at the end of the testing was noted to help assess the failure mode.

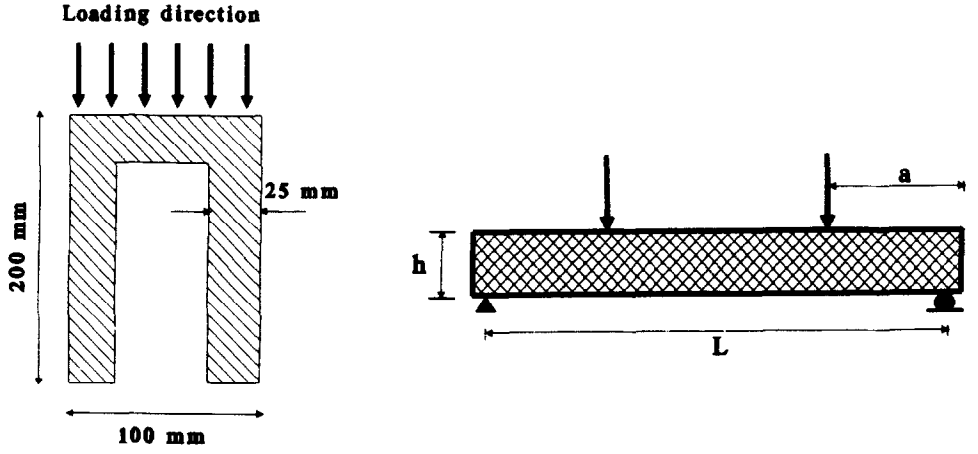

Figure 1: *Specimen dimensions and loading configuration*

Influence of Major Parameters on Cracking Shear Strength

Plots were obtained for all the specimens tested for the load versus the center point deflections (V-d_c) for the different parameters under investigation. Typical V-d_c curves are shown in Figures 2, 4 and 6 for the effect of volume fraction, a/h ratio and mortar strengths. The presence of only two distinct stages in the curves, that of a quasi-linear behavior before cracking and a nonlinear behavior after cracking, without any significant plastic deformational nonlinearity at the ultimate stage, indicate that the beams failed primarily in shear or shear-flexure but not due to pure flexure. The beam designations, material properties and test results are summarized in Table 1. The beams are designated according to the following general notational expression, XYn, where X indicates the shear span to depth ratio (varies from A to C), Y indicates the water cement ratio in terms of mortar strength, and n indicates the number of wire mesh layers in terms of volume fraction.

Effect of Amount of Wire Mesh Reinforcement

The effect of the volume of reinforcement V_f, in the form of number of wire mesh layers, on the first cracking strength and ultimate shear capacity are shown for a representative sample in Figure 2. The following expression is used to calculate V_f

$$V_f = \frac{\pi d_b^2 (N_f b_f + 2 N_w h)}{4D (b_f t_f + 2 h t_w - 2 t_f t_w)}$$

where d_b and D are wire mesh diameter and opening, respectively; N_f and N_w are number of wire mesh layers in the flanges and webs; b_f and t_f are flange width and thickness, respectively; h is the beam depth and t_w is the web thickness.

The increase in V_f clearly indicates an increase in the cracking shear strength, for any given value of a/h

ratio and f'_c. An increase in ductility is also evident, associated with the improved shear strength. In general, the crack resistance of ferrocement is found to be much larger than ordinary reinforced concrete due to the dispersed wire meshes which increases the tensile strength of the material as a whole.

The variation of the cracking shear strength ($v_{cr}=V_{cr}/b_w h$) with amount of reinforcement V_f, is shown in Figure 3. An empirical expression for v_{cr} as a function of V_f, a/h ratio and f'_c has developed and is discussed in a later section.

TABLE 1: Beam designations, material properties and test results.

Specimen	f'_c (MPa)	f_t (MPa)	V_f	a / h	v_{cr} (kN)
AII1	41.72	4.0	0.00445	1.5	14.0
AII2	41.72	4.0	0.00889	1.5	17.0
AII3	41.72	4.0	0.0134	1.5	18.5
BI1	36.88	3.9	0.00445	2.0	12.0
BI2	36.88	3.9	0.00889	2.0	15.0
BI3	36.88	3.9	0.0134	2.0	16.5
BII1	44.31	4.5	0.00445	2.0	12.5
BII2	44.31	4.5	0.00889	2.0	15.5
BII3	44.31	4.5	0.0134	2.0	17.5
CI1	44.89	4.4	0.00445	2.5	9.5
CI2	44.89	4.4	0.00889	2.5	12.0
CI3	44.89	4.4	0.0134	2.5	15.0
CII1	40.62	4.3	0.00445	2.5	10.5
CII2	40.62	4.3	0.00889	2.5	13.0
CII3	40.62	4.3	0.0134	2.5	14.0

Effect of Shear Span to depth Ratio (*a/h*)

The effect of shear span to depth ratio on the load-deflection curve and consequent cracking and ultimate shear strength of ferrocement beams is shown for typical specimens in Figure 4. The increase in a/h ratio reduces the cracking strength and the shear strength, as evident in Figure 5, and the mode of failure changes from pure web cracking to flexure-shear cracking as witnessed from the cracking patterns monitored in the tests. The a/h ratio is therefore the most important parameter governing the failure mode. However the failure mode might change for a given a/h ratio depending upon the amount

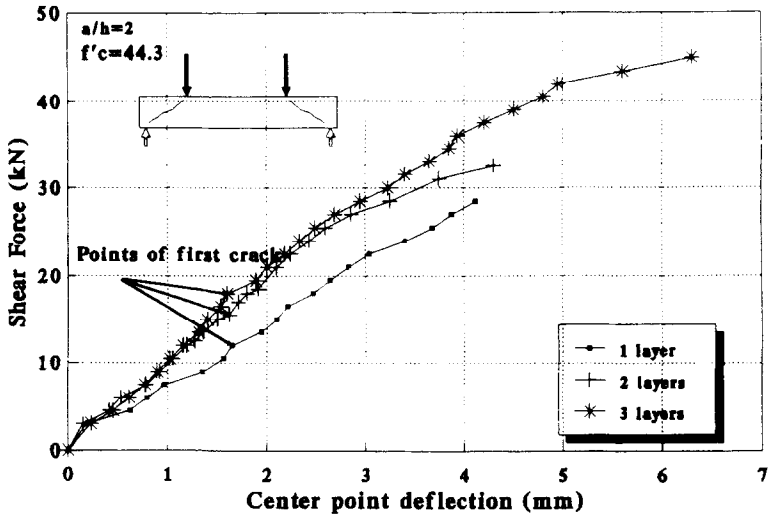

Figure 2: *Typical load-deflection curve showing the effect of wire mesh reinforcement*

of wire mesh reinforcement. Crack patterns at failure are strongly influenced by the *a/h* ratio, originating as diagonal shear cracks near the mid-depth of the section for *a/h* values of 1.5; originating near the lower third for *a/h* values of 2.0; and flexural cracks at the bottom fibers for *a/h* values of 2.5. In all cases, considerable reserve strength is obtained after the first crack, with the propagation of cracks diagonally towards both the top and bottom of the beam between the applied load and support locations, with increase in load. Also new cracks are initiated with increasing load and existing cracks show dilatancy.

Effect of Mortar Compressive Strength

The effect of mortar compressive strength, f'_c, on the load-displacement behavior of typical specimens

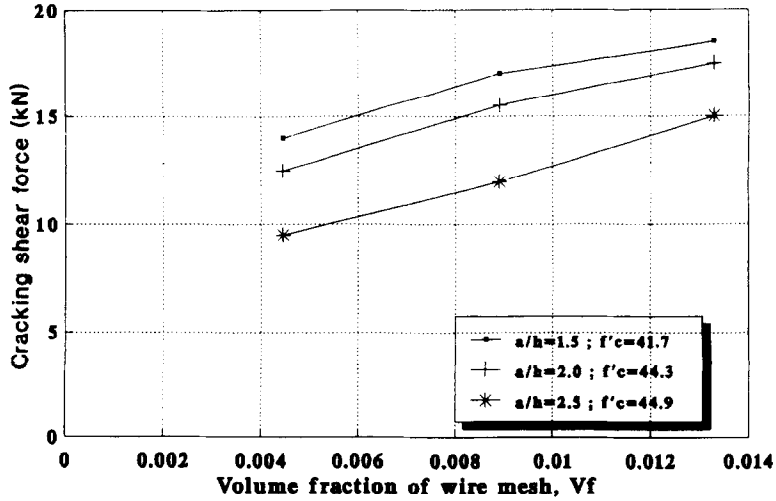

Figure 3: *Effect of wire mesh reinforcement on cracking shear strength*

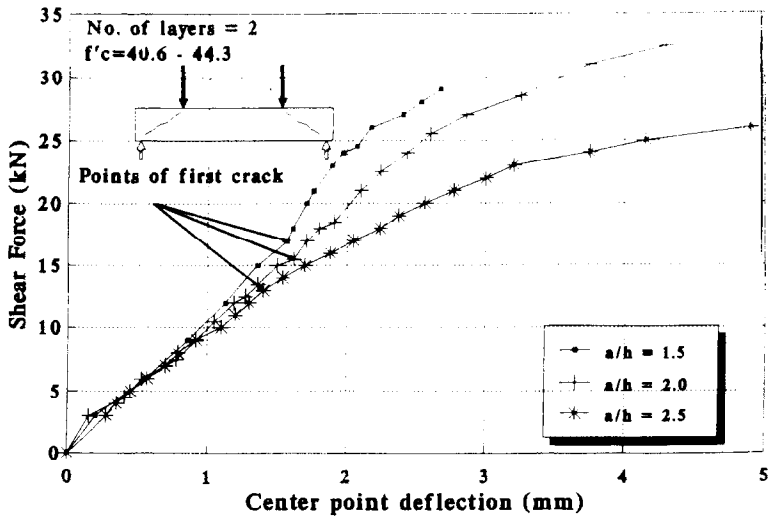

Figure 4: *Typical load-deflection curves showing effect of a/h ratio*

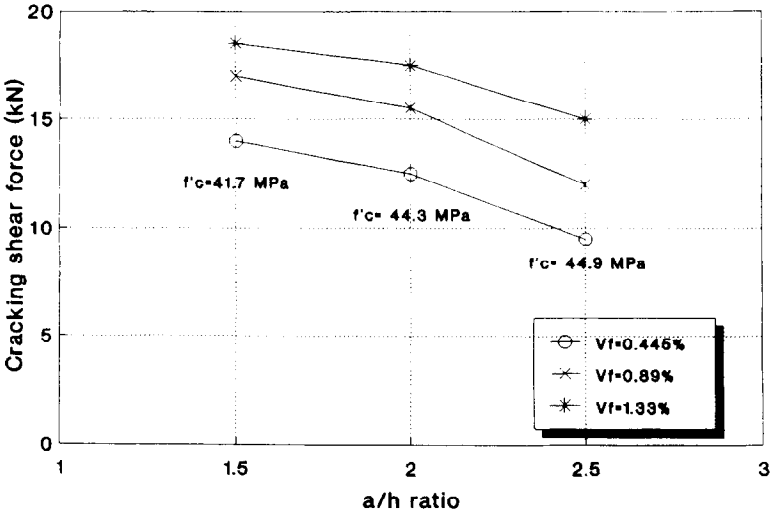

Figure 5: *Effect of a/h ratio on cracking shear strength*

is shown in Figure 6. Increase in f'_c results in an increase in both cracking and ultimate shear strengths, and also the ductility of the specimen. However, large variations in mortar strength could not be very successfully simulated for the water cement ratio range of this study. More tests are required to observe the effect of a large variation of f'_c on v_{cr}.

Modelling of Cracking Shear Strength

As discussed before, cracking shear strength can be considered to be one of the limiting design conditions where crack-free structural behavior is desired. Therefore it is imperative to propose a computational model to predict the cracking shear strength for ferrocement sections.

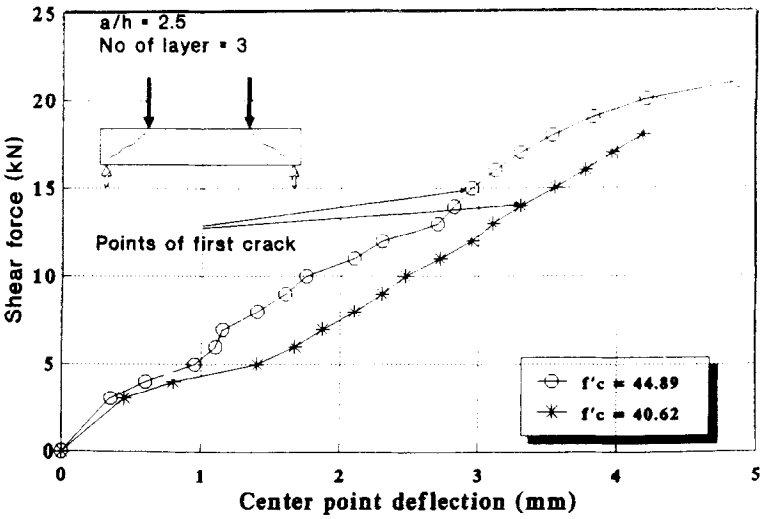

Figure 6: *Typical load-deflection curve showing effect of mortar compressive strength*

The tensile strength is normally ignored in conventional reinforced concrete design but still its contribution is not overlooked in research studies. Ferrocement on the other hand shows a much improved behavior in tension, it would thus not only be an over simplification by neglecting the tensile strength of ferrocement but would be totally unjust, and a complete under estimate of a very significant contribution of tensile strength. The computational model developed in this study therefore, emphasizes the tensile strength contribution in the cracking limit state.

Although strictly speaking ferrocement is a non-linear, non-homogenous material, before the initiation of first crack it can be idealized for modelling to have elastic homogenous material behavior. Using the Euler-Kirchoff hypothesis of plane sections remaining plane before and after bending, we have, for combined effects of shear stresses and flexure stresses, the principle stresses s_1 and s_2 given by

$$\sigma_{12} = \frac{\sigma_x + \sigma_y}{2} \pm \sqrt{\frac{(\sigma_x - \sigma_y)^2}{4} + \tau_{xy}^2}$$

where, s_x , s_y are the intensities of the normal fiber stresses along and perpendicular to the local beam axis, and t_{xy} is the intensity of the tangential shear stress. The inclined principal stresses make an angle a with the horizontal such that

$$\tan \alpha = \frac{\tau_{xy}}{(\sigma_x - \sigma_y)}$$

In an ordinary beam problem, the presence of normal stress perpendicular to the beam axis, s_y, can be neglected. The distribution profile of the horizontal flexure stresses at any point in the cross section is then represented by

$$\sigma_x = \frac{My}{I}$$

where s is the bending stress at a distance y from the neutral axis. M is the bending moment at the section and I is the moment of inertia of the cross section at neutral axis.

The shear stress distribution profile of uncracked ferrocement section is computed based on the elastic beam theory for homogenous beams.

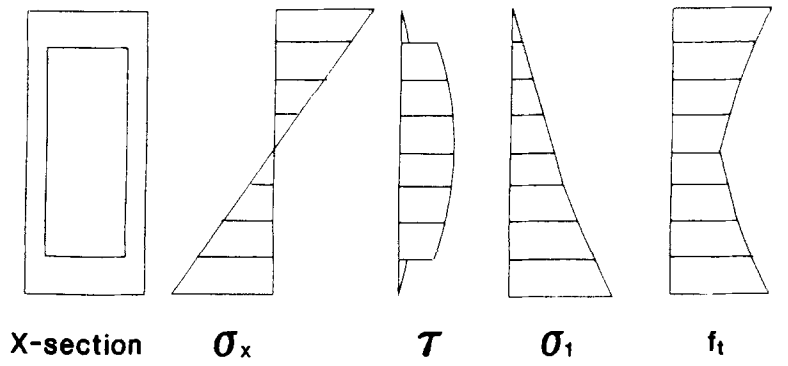

Figure 7: *Distribution of flexural, shear, principle tensile and allowable tensile stress profiles across the section*

Then, the shear stress t_{xy} at any point in the cross section is given by

$$\tau_{xy} = \frac{V}{I} \int_{y_1}^{c} \frac{y\, dA(x,y)}{b(y)}$$

where V is the vertical shear force, b is the sectional width and $\grave{o}ydA$ is the sum of the moment of the differential areas about the neutral axis.

By modelling the distribution of flexure and shear stresses based on the Euler-Kirchoff hypothesis across the depth of the cross-section the intensity and direction of the principal tensile stresses can be computed, and compared to the tensile strength of ferrocement, which is taken as the cracking criteria. This is shown in Figure 7 for a generic cross-sectional shape.

Quite a few number of research has been done previously to determine the first cracking tensile strength of ferrocement [11,12,13,14]. These show that similar to reinforced concrete the modulus of rupture indicates a higher value of tensile strength than direct axial tension tests, owing to material nonlinearity and localized stress redistribution prior to tensile cracking. The tensile strength relations are obtained from references [11,12] which gives

$$f_{t'} = 24.52\, S_L + f_t$$

$$f_{r'} = 280.2\, S_L + f_r$$

where f'_t, f'_r, f_t and f_r are the axial tensile strength and modulus of rupture of ferrocement and plain mortar respectively; S_L is the specific surface of the reinforcement, defined as the total surface area of the reinforcement per unit volume of the section (1/mm).

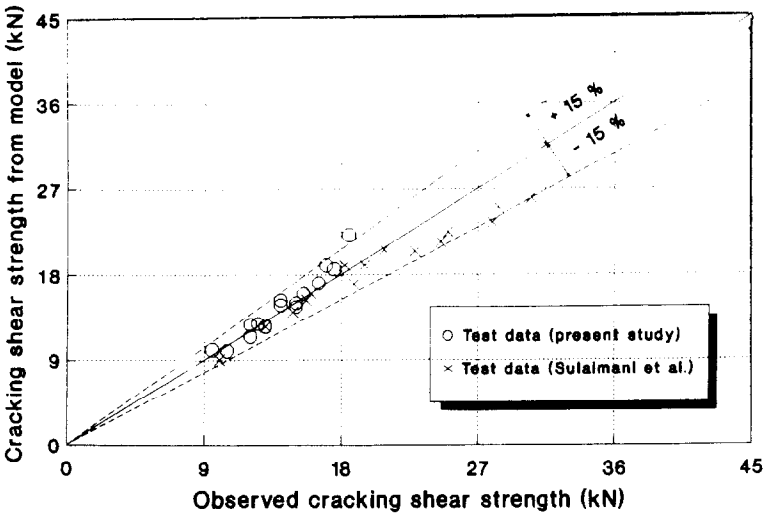

Figure 8: *Comparison of experimental and proposed model results for cracking shear strength*

In view of this phenomenon, the cracking criteria established in the present model, relates the tensile strength at the neutral axis to the axial tensile strength of ferrocement and that at the outer most fiber to the modulus of rupture. The profile of distribution of tensile strength is then idealized by a second degree parabolic variation, between these two limits, as shown in Figure 7. Using this simple approach, and discretizing the cross section into finite number of small two dimensional elements, computations were carried out for comparison of the first cracking loads for results of tests conducted for this study and results of box beams reported by Sulaimani et al. [10]. (The modulus of rupture, not reported, for these test results were assumed as twice the axial tensile strength for mortar). The results are plotted in Figure 8, and the model results show satisfactory correlation with the test results. The coefficient of variation of the ratio between model and experimental results for thirty test data (fifteen each from this study and [10]) is 8.3% with a mean value of 1.024.

Since the above procedure involves the determination of critical tensile principle stresses across the section depth, involving discretization and computation for different layers, a simpler empirical expression is also proposed which can be used directly to predict v_{cr}. In an attempt to develop such an expression for ferrocement thin webbed sections over the entire range of parameters studied under this research, a multiple regression analysis was conducted for different forms of expressions and the following form gives the best fit, for the range of the parameters of the tested beams.

$$v_{cr} = K \left(f_{c'} \frac{h}{a} V_f \right)^n$$

where, f'_c is the mortar compressive strength, a/h is the shear span to depth ratio and V_f is the volume fraction of the wire mesh reinforcement. For the best fit of the experimental results the values of K and n obtained were 2.6511 and 0.3549, respectively, with an adjusted coefficient of determination R^2 equal to 0.946. The final expression proposed thus becomes,

$$v_{cr} = 2.65 \left(f_{c'} \frac{h}{a} V_f \right)^{0355}$$

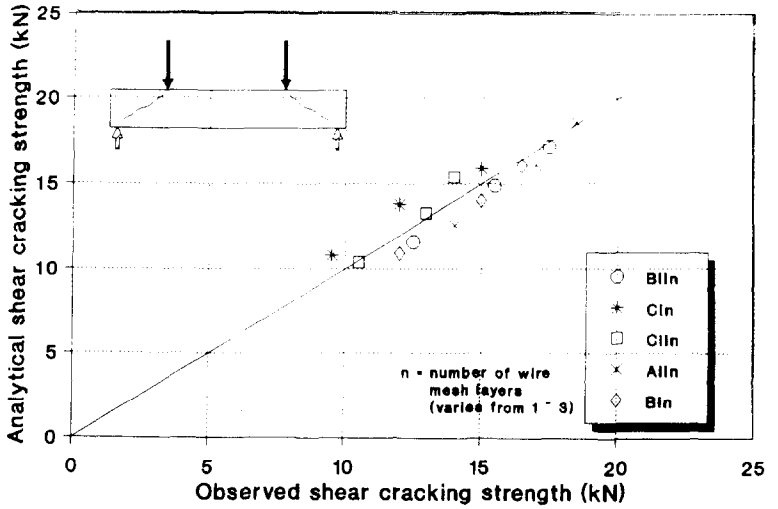

Figure 9: *Comparison of experimental cracking strength and proposed expression results*

A plot of the model results for v_{cr} and the experimentally obtained values for the present study are shown in Figure 9, showing the validity of the form of the proposed expression.

Conclusions

Based on the test results of thin webbed channel beams under transverse shear loads, and the computational model and empirical expression proposed, the following conclusions can be drawn

1) The cracking and ultimate shear strength of ferrocement channel beams increases as the shear span to depth ratio decreases and / or the amount of wire mesh or mortar strength increases.

2) Unlike conventional reinforced concrete without shear reinforcement, web cracking in ferrocement beams do not indicate ultimate strength, and sufficient reserve strength and ductility remains even after cracking occurs. In general, two distinct phases of load deflection behavior is witnessed with respect to pre and post cracking.

3) The crack initiation and failure mechanism of ferrocement beams are closely associated with shear span to depth ratio. At shear span to depth ratio $\leq$ 2.0, first cracking usually occurs near the mid depth of the section; whereas bottom fibre flexural cracks appear first at higher shear span to depth ratios.

4) By suitably modelling the tensile strength variation across the depth of the beam, a simple computational model, based on elastic homogenous beam theory, can be successfully utilized to predict first cracking shear strength of ferrocement beams of any generic cross-sectional shape.

5) An empirical expression is also proposed to predict the first cracking shear strength of ferrocement channel beams. The proposed equation is however valid within the range of parameter of the tested beam.

Notations

a	Shear span
a/h	Shear span to beam depth ratio
b_f	Flange width
b_w	Thickness of both webs of section
c	Depth of neutral axis
d_b	Wire mesh diameter
D	Wire mesh opening
f'_c	Mortar compressive strength (MPa)
f_r	Mortar modulus of rupture (MPa)
f_t	Mortar tensile strength (MPa)
f'_r	Ferrocement modulus of rupture (MPa)
f'_t	Ferrocement tensile strength (MPa)
h	Over all beam depth
I	Moment of inertia
M	Bending moment
N_f	Number of wire mesh layers in flange
N_w	Number of wire mesh layers in each web
S_L	Specific surface of wire mesh (1/mm)
t_f	Flange thickness
t_w	Web thickness
v_{cr}	Cracking shear strength of ferrocement (MPa)
V	Shear force
V_{cr}	Cracking shear force
V_f	Volume fraction of wire mesh
y	Distance of element from neutral axis
α	Angle of inclination of principle plane with horizontal axis
δ_c	Beam mid span deflection
$\sigma_{x,y}$	Flexural stresses
$\sigma_{1,2}$	Principle tensile, compressive stresses
τ_{xy}	Vertical shear stresses

References

1) *"State of the Art: Report on Ferrocement"*, **ACI**, Committee 594, 1982.

2) Paul, B. K. and Pama, R. P., *"Ferrocement"*, **IFIC**, AIT, Bangkok, 1978.

3) *"Ferrocement Material and Application"*, **ACI**, SP-61, 1979.

4) Basunbul, I. A., Al-Mandil, M. Y. and Al-Sulaimani, G. J., *"Study and Design of Ferrocement Structural Systems"*, **KACST**, Reports No. 1,2,3 and 4, July 1984 - Sept. 1985.

5) Al-Sulaimani, G. J., Ahmad, S. F. and Basunbul, I. A., *"Study of Flexural Strength of Ferrocement Flanged Beams"*, **Arabian Journal for Science and Engineering**, vol. 14(1), Jan. 1989, pp. 33-46.

6) Balaguru, P. N., Namaan, A. E. and Shah, S. P., *"Analysis and Behavior of Ferrocement in Flexure"*, **Journal of Struct. Div., ASCE** 103, ST10, Oct. 1977, pp. 1937-1949.

7) Al-Sulaimani, G. J. and Basunbul, I. A., *"Behavior of Ferrocement under Direct Shear"*, **Journal of Ferrocement**, vol. 21, No. 2, April 1991, pp. 109-117.

8) Mansur, M. A. and Ong, K. C. G., *"Shear Strength of Ferrocement Beams"*, **ACI Structural Journal**, 84-S2, Jan.-Feb. 1987, pp. 10-17.

9) Mansur, M. A. and Ong, K. C. G., *"Shear Strength of Ferrocement I-Beams"*, **ACI Structural Journal**, 88-S48, July-Aug. 1991, pp. 458-464.

10) Al-Sulaimani, G. J., Basunbul, I. A. and Mousselhy, E. A., *"Shear Behavior of Ferrocement Box Sections"*, **Cement and Concrete Composites** 13, 1991, pp. 29-36.

11) Naaman, A.E., *"Reinforcing Mechanisms in Ferrocement"*, **M.S. Thesis**, Massachusetts Institute of Technology, Sept 1970.

12) Logan, D, Shah, S. P., *"Moment Capacity and Carrying Behavior of Ferrocement in Flexure"*, **ACI Journal**, Proc., vol. 70, No., 12, Dec. 1973, pp. 799-804.

13) Johnston, C. D., and Matter, S. G., *"Ferrocement in Compression and Tension"*, **Jour. of Structural Div.**, ASCE, vol. 102, ST 5, May 1976, pp. 875-899.

14) Naaman, A. E., and Shah, S. P., *"Tensile Tests of Ferrocement"*, **ACI Jour.**, vol 68, No. 9, Sept. 1971, pp. 693-698.